Design of inverted-F antenna for long-term evolution-based wireless handheld devices

Paulkani IYAMPALAM[*], **Indumathi GANESAN**
Department of Electronics and Communication Engineering, Mepco Schlenk Engineering College, Sivakasi,
Tamil Nadu, India

Abstract: In this article, a compact triple-band inverted-F antenna for long-term evolution (LTE)-based wireless handheld devices is presented. The proposed antenna comprises three arms, namely the radiating arm, shorting arm, and feeding arm. The structure of the designed antenna looks like an inverted F with folded L-shaped strip antenna. It has three resonant frequencies of 795, 2050, and 3405 MHz with a reflection coefficient of –11.7 dB, –15.1 dB, and –30.5 dB, respectively. The size of the suggested antenna is $10 \times 35 \times 0.8$ mm^3 and it is built on the FR-4 substrate which is more compact and easy to integrate with the handheld devices such as laptops, tablets, and smart phones. The performances of the proposed antenna are analyzed with the help of computer simulation using Ansys High Frequency Structure Simulation Software Simulator (HFSS). The measured –10 dB impedance bandwidth of the suggested antenna covers 780–820, 2020–2070, and 3230–3490 MHz, which satisfies the LTE 700, LTE 2100, and LTE 3300. The proposed antenna has the acceptable voltage standing wave ratio (VSWR $\leq$ 2), bandwidth, gain, and radiation characteristics across the operating bands and thus proves its suitability for wireless handheld devices.

Key words: Inverted-F antenna, long-term evolution, triple-band, wireless handheld devices

1. Introduction

With the expeditious development of wireless communication systems, there is a significant interest in providing more compact, small-size, and multiband antennas in wireless handheld devices. However, designing an internal compact antenna for multiple bands of long-term evolution (LTE) service in small handsets is still a serious challenge for the laptop, tablet and smart phones. Such internal antennas are required to cover the frequency bands of LTE 700, GSM850 (824–894 MHz), GSM900 (880–960 MHz), GPS (1575 MHz), DCS (1710–1880 MHz), PCS (1850–1990 MHz), UMTS (1920–2170 MHz), LTE 2300 and wireless local area network (WLAN) (2400–2484 MHz). In addition, the internal antenna should be lightweight, low-profile, low-cost, and small in size. Artificial materials are integrated with the microstrip antennas to realize the electrically small antennas [1]. Nowadays, LTE operation for the 4G communications is more popular because of its high data rate. The LTE standard starts from 698 MHz and goes up to 3800 MHz. There are various types of antennas proposed like planar inverted-F antenna [2–4], monopole [5, 6], loop [7] antenna folded monopole/dipole/loop [8] antennas for covering LTE applications. Among these antennas, the combination of the loop and inverted-F antenna (IFA) is generally used for the internal antenna due to its low profile, low cost, and easy fabrication.

Park and Sung proposed a reconfigurable antenna with the size of $45 \times 11 \times 6$ mm^3 for mobile handsets

---

[*]Correspondence: paulkani64@gmail.com

[9]. It is operated in quad-band for GSM900/GSM1800/GSM1900 and UMTS applications. The authors contributed hepta-band reconfigurable folded loop-inverted-F antenna for GSM850, GSM900, GPS, DCS, PCS, UMTS, and WLAN applications in [10]. It consists of Philips BAP64-03 silicon PIN diode, biasing circuit, and matching bridge to achieve high bandwidth. In [11], the authors proposed eight-band antenna with a single-pole four-throw RF switch which is designed for LTE/WWAN tablet computer applications. An antenna for GNSS, lower WiMAX, WLAN, and X-band applications is designed in [12]. The frequency reconfigurablity mechanism and trapezoidal slot structure are used to attain four bands. To achieve a multiband behavior, monopole antenna with multiple branches and tuning circuits are embedded in the radiating patches for mobile handset [13, 14]. At present, some of the multiband antennas are designed for mobile phone [15–17] and tablet applications [18–20]. Recently, a large number of antennas have been reported for triple-band operation [18–22]. Although multiband is achieved by these antennas, there is still a limitation regarding VSWR. In the above-mentioned antennas, the frequency coverage is defined by a VSWR which is less than 3 (VSWR 3:1). It indicates that the power delivered to the antenna is only 50% if VSWR is considered to be less than 3 (reflection coefficient below –6 dB) and the impedance match of the antenna is very poor. The remaining 50% power is reflected. To overcome these problems, we propose a triple-band antenna with VSWR less than 2. In this case, the power delivered to the antenna can be 90% since the reflection coefficient of an antenna is considered to be less than –10 dB.

In this work, a compact LTE triple-band antenna design for portable wireless devices is proposed. Three branches called the shorting arm, radiating arm, and feeding arm are printed on the FR-4 substrate. It has the dimension of $10 \times 35 \times 0.8$ mm^3. Furthermore, the prototype of the antenna is fabricated and optimised using ANSYS HFSS v17.

2. Antenna design

Figure 1 shows the geometry of the proposed inverted-F antenna (IFA) for LTE applications. It has a inverted-F and L-shaped structure, including a radiating arm, feeding arm, shorting arm, and ground pad. It is constructed on a thin flame retardant glass reinforced epoxy resin (FR-4) substrate of thickness 0.8 mm, relative permittivity (ϵ_r) of 4.4, and loss tangent of 0.024. It has a volume of $10 \times 35 \times 0.8$ mm^3. The female SMA connector is used to feed the signal to the antenna. The size of the device ground plane (bottom layer) is 150×200 mm^2. The selected dimensions are for a 9.7-inch tablet computer. The resonant frequency (f_r) of the proposed IFA is calculated by the following eqution [23]:

$$f_r = \frac{c}{4 * (L + W) * \sqrt{\epsilon_r}},$$ (1)

where L and W are respectively the length and width of the antenna, ϵ_r is the dielectric constant of the substrate, and c is the free space speed of light.

Here, the variables L_S, W_S, L_{R1}, L_{R2}, W_{R1}, W_{R2}, L_{R3}, and L_{R4} for radiating arm, W_{S1}, L_{S1}, W_{S2}, L_{S2}, and W_{S3} for feeding arm, and L_{F1}, W_{F1}, L_{F2}, W_{F2}, L_{F3}, W_{F3}, L_{F4}, W_{F4}, L_{F5}, and W_{F5} for shorting arm are used to represent the dimensions of the proposed antenna. In order to get optimum results for achieving desired LTE bands, parametric analysis have been performed by using ANSYS HFSS v17 software. The optimized results are listed in Table 1. The design evolution of the suggested antenna is demonstrated in Figure 2.

The first stage starts with the basic inverted-F antenna as shown in configuration "Antenna I"of Figure 2a. The radiating arm of the IFA is folded to provide the compact size. In order to achieve LTE middle band, the
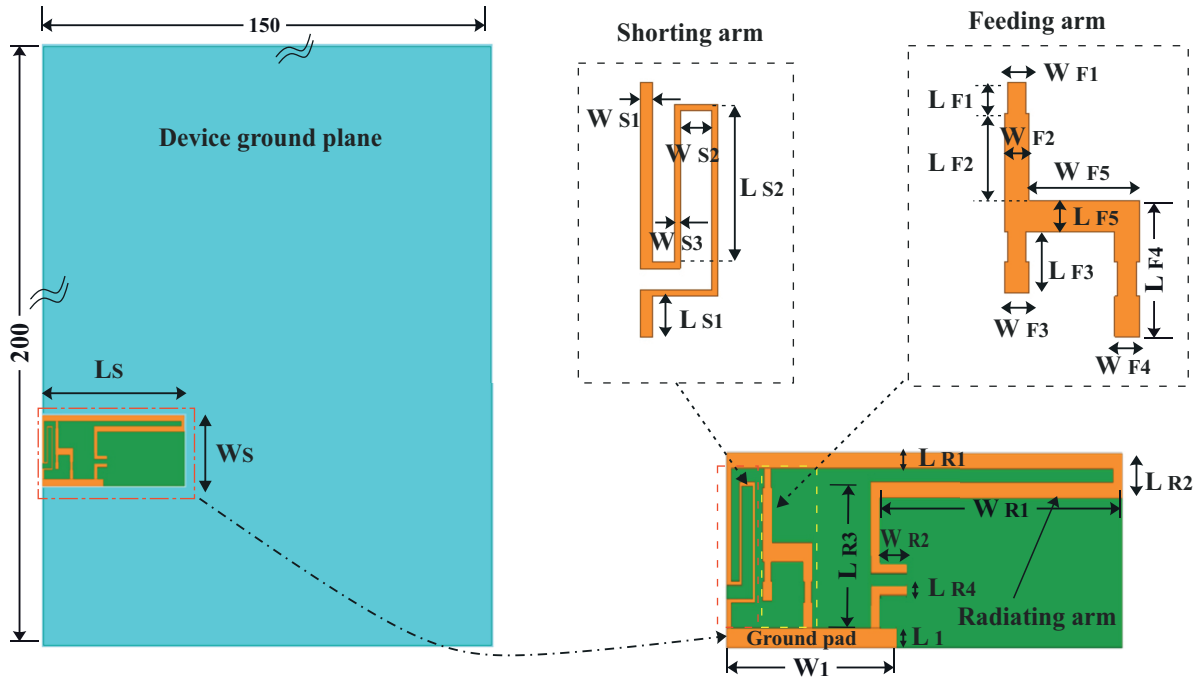
Figure 1. Geometry of the proposed inverted-F antenna with ground plane and enlarged view of the antenna structure.

Table 1. Dimensions of the proposed antenna.

Parameters	Value (mm)	Parameters	Value (mm)	Parameters	Value (mm)	Parameters	Value (mm)
L_S	10	W_S	35	L_{R1}, W_{F2}, W_{F3}	0.8	W_{R1}	21.5
L_{R2}	2.3	W_{R2}	2.5	L_{R3}	7.5	L_{R4}	0.5
L_{S1}	1.3	W_{S1}	0.4	W_{S2}, L_{F1}, L_{F5}	1	L_{S2}	5.1
W_{S3}	0.2	W_{F1}, W_{F4}	0.6	L_{F2}	2.8	L_{F3}	2
L_{F4}	4.4	W_{F5}	3.55	L_1	1	W_1	15

shorting arm of the IFA is modified by adding a loop strip as depicted in Figure 2b. After that, the reflection coefficients of "Antenna II"are –15.48 dB at 2180 MHz and –7.38 dB at 2960 MHz. This antenna does not meet the desired frequency bands. As seen in Figure 2c, the L-shaped strip is employed in the feeding arm to enhance the bandwidth in the LTE middle band (2010–2025 MHz). The "Antenna III"operates at three frequencies of 2180, 3490, and 3629 MHz and the corresponding reflection coefficients are –18.7 dB, –13.4 dB, and -14.32 dB. Although the antenna covers LTE middle band and LTE high band, LTE low band is not obtained. Finally, the two parallel microstrip lines are added in the open end of the radiating arm. At high frequency, these parallel lines act as a capacitor and improve the excited surface current distributions on the radiating arm. This enhances the bandwidth of the antenna's high band and leads to the antenna resonant at the LTE low band (788–798 MHz). The configuration of the proposed inverted-F antenna is presented in Figure 2d. The length (L_S) of 10 mm and the width (W_S) of 35 mm are taken as the initial dimension for the resonant frequency of 794.5 MHz, which belongs to LTE 700 band (low band) but "Antenna I"exhibits a dual-resonant behavior at 1320 and 2420 MHz.

The surface current distribution on the antenna is shown in Figure 3. Findings show that the maximum current flow exists on the folded structure in the radiating arm. The total length of the folded radiating arm
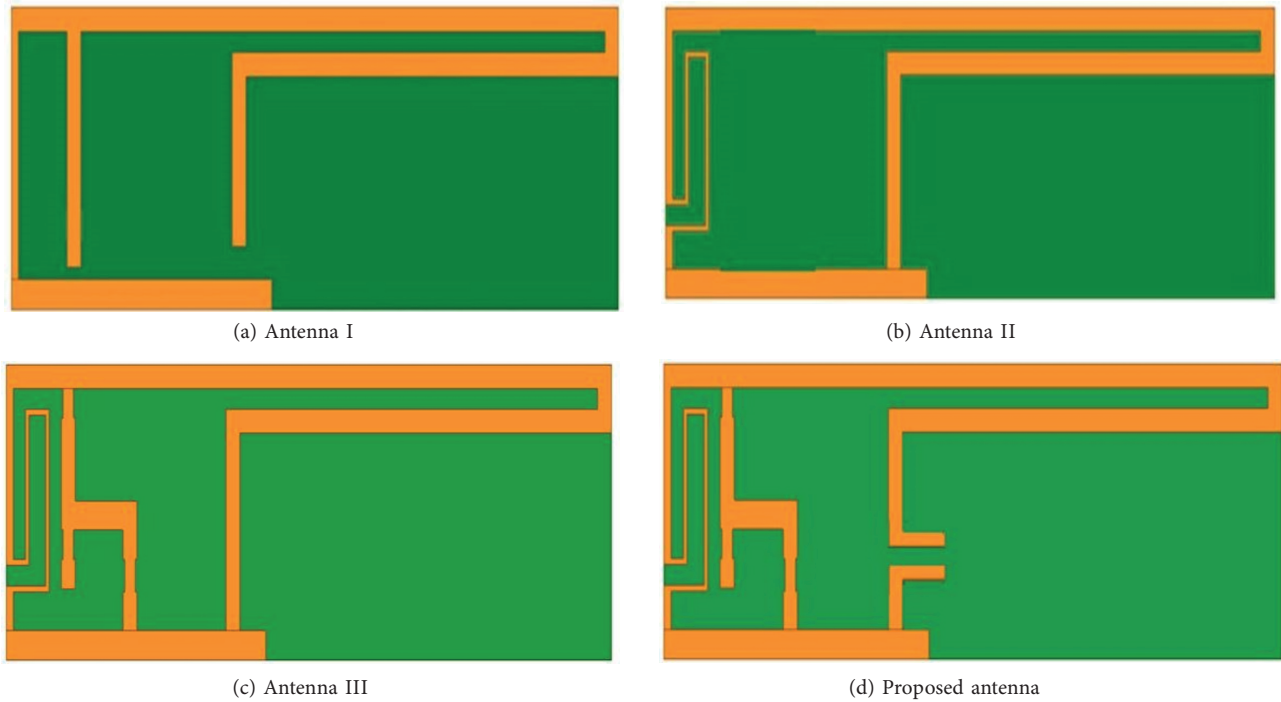
(a) Antenna I

(b) Antenna II

(c) Antenna III

(d) Proposed antenna

Figure 2. Evolution stages in the proposed inverted-F antenna design.

from point 'd', through points 'e' and 'f' then to point 'g' in Figure 3a (35 mm + 2.3 mm + 21.5 mm + 3.7 mm = 62.5 mm) is close to 0.25 wavelength at 1320 MHz. This allows the antenna to resonante at 1320 MHz. Similarly, the additional resonant mode occurred at 2420 MHz. Thus, the total length of the feeding arm and shorting arm from point 'h'through 'i', 'j', and 'k'(7 mm + 1 mm + 0.4 mm + 9 mm + 3.6 mm + 0.8 mm + 6.8 mm + 0.8 mm = 29.4 mm) is still close to 0.25 wavelength at 2420 MHz, which is depicted in Figure 3b.

3. Simulated results and discussions

The antenna structure is validated using Ansys HFSS software, which uses the principle of finite element method analysis. Figure 4 illustrates the simulated reflection coefficient spectrum of Antenna I, Antenna II, Antenna III, and the proposed inverted-F antenna. It is found that the proposed IFA can cover the desired LTE frequency band. In the simulation, the first resonance appears at 747 MHz with the bandwidth of 4.02% from 730 to 760 MHz (30 MHz) and the reflection coefficient of –11.73 dB. The proposed antenna covers LTE middle band from 1950 to 2030 MHz with the 4.04% (80 MHz centred at 1985 MHz) impedance bandwidth and –12.10 dB reflection coefficient. In the LTE high band, the high bandwidth of 13.74% from 3180 to 3650 MHz (470 MHz) with better reflection coefficient is obtained at 3425 MHz.

4. Parametric study

The parametric analysis of the proposed IFA is performed in order to get optimized results for LTE operation. The study is done by varying length and width of the substrate and radiator dimensions like L_S, W_S, L_1, W_1, and W_{R1} while keeping other dimensions constant.
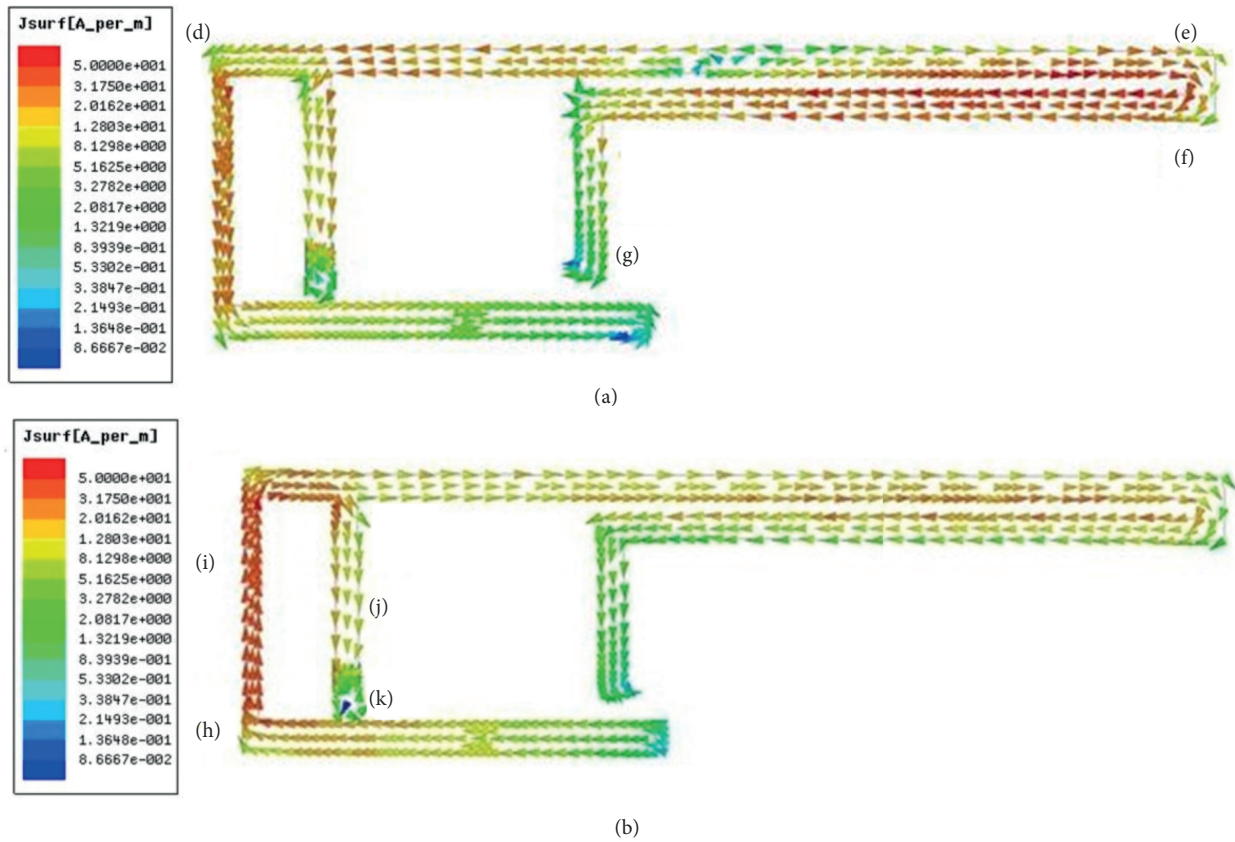
Figure 3. Vector surface current distribution of Antenna I at (a) 1320 MHz, (b) 2420 MHz.

4.1. Effect of length and width of the substrate

Figure 5 shows the simulated reflection coefficient spectrum for different length (L_S) of the substrate with other parameters remaining fixed. The length (L_S) is varied from 10 to 14 mm. The frequency is shifted to the higher value as the length of the substrate increases.

It is observed that the best result is achieved at $(L_S) = 10$ mm. Therefore, the length of the substrate (L_S) is taken as 10 mm. The simulated reflection coefficient spectrum for different width (W_S) of the substrate is depicted in Figure 6. It is observed that the frequency decreases when the width of the substrate increases. At $W_S = 35$ mm, the suggested antenna covers the required triple band for LTE operations.

4.2. Effect of length and width of the ground pad

The length and width of the ground pad are varied and its effect is observed. The simulated reflection coefficient for various length L_1 and width W_1 are illustrated in Figures 7 and 8. The values of width L_1 and width W_1 vary from 0.5 to 1 mm and 10 to 15 mm, respectively. The desired operating frequency can be achieved with a length (L_1) of 1 mm and width (W_1) of 15 mm.

Figure 9 describes the reflection coefficient results for the proposed antenna in terms of length (W_{R1}). As W_{R1} increases from 0.1 to 0.5 mm with other parameters remaining fixed, it is found that the frequency shifts at the higher band. The antenna has the desired band at $W_{R1} = 21.5$ mm. Based on the parametric analysis, the optimum values of the antenna are selected.
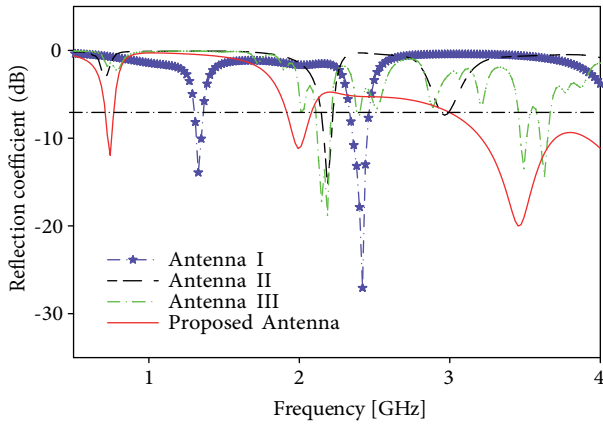
Figure 4. Simulated reflection coefficient spectrum of Antenna I, Antenna II, Antenna III, and the proposed antenna.
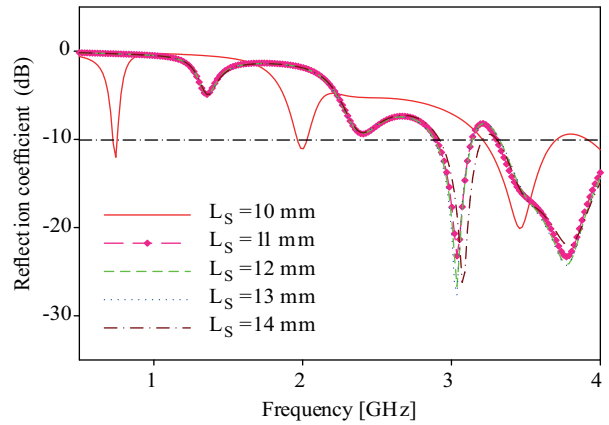

Figure 5. Reflection coefficient spectrum of the IFA antenna for different lengths (L_S) ranging from 10 to 14 mm.
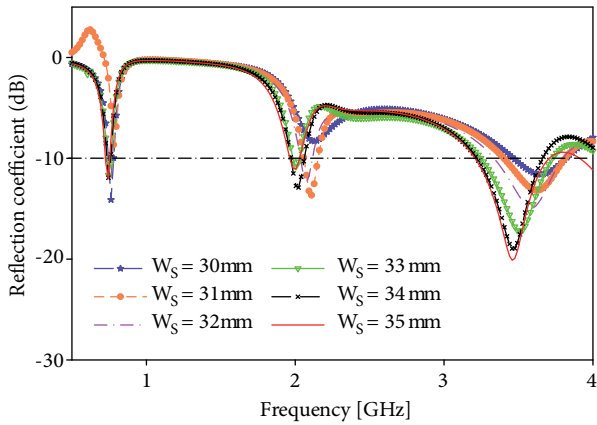

Figure 6. Reflection coefficient spectrum of the IFA for different widths (W_S) ranging from 30 to 35 mm.
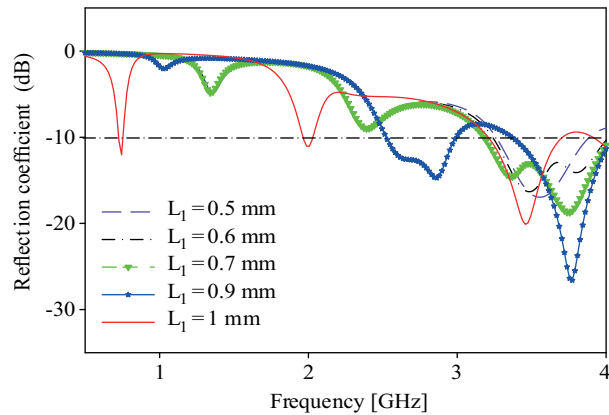

Figure 7. Reflection coefficient spectrum of the IFA for different lengths (L_1) ranging from 0.5 to 1 mm.
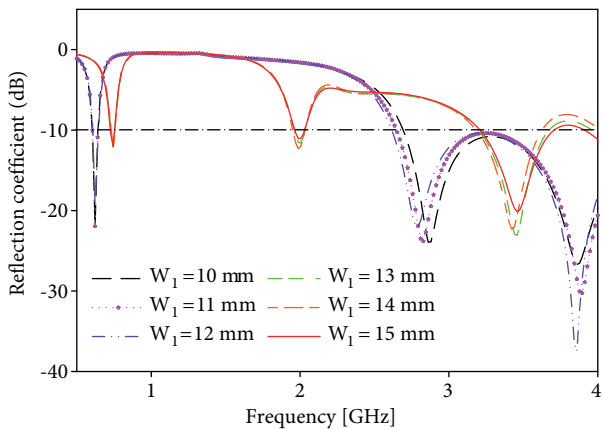

Figure 8. Reflection coefficient spectrum of the IFA for different widths (W_1) ranging from 10 to 15 mm.
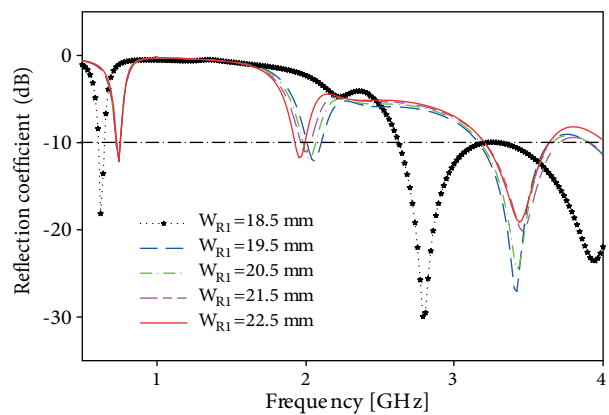

Figure 9. Reflection coefficient spectrum of the IFA for different widths (W_{R1}) ranging from 18.5 to 22.5 mm.

5. Measured results and discussions

In order to verify the simulation results, the proposed antenna is fabricated and tested. The fabricated antenna is mounted on the corner of the device ground plane (9.7-inch tablet device). PCB edge mountable female SMA connector is used for exciting the antenna. The centre lead of the SMA connector is connected to the antenna feed point through wire and the negative terminal is connected to the device ground plane. The photograph of the fabricated antenna is depicted in Figure 10. Figure 11 illustrates the measured and simulated reflection coefficient characteristics of the designed antenna.

It has a triple band with an impedance bandwidth of 40 MHz or 5.03% in the LTE low band from 780 to 820 MHz (centered at 795 MHz), 50 MHz or 2.43% in the LTE middle band from 2020 to 2070 MHz (centered at 2050 MHz) and 260 MHz or 7.63% in the LTE high band from 3230 to 3490 MHz (centered at 3405 MHz) respectively. The corresponding reflection coefficients of the suggested antenna are –11.7 dB at 795 MHz, –15.1 dB at 2050 MHz, and –30.5 dB at 3405 MHz. It is evident that the designed antenna has acceptable reflection coefficient characteristics over the operating bands. The differences between the simulated and measured results are 48, 65, and 20 MHz. This difference occurred due to the inaccuracy in the fabrication and manual soldering of the antenna prototype.
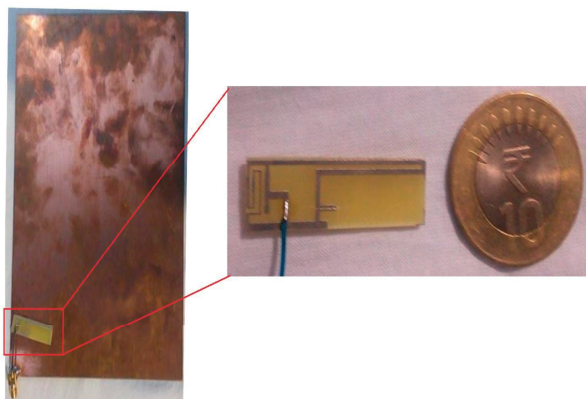

Figure 10. Photograph of the fabricated prototype of the inverted-F antenna.
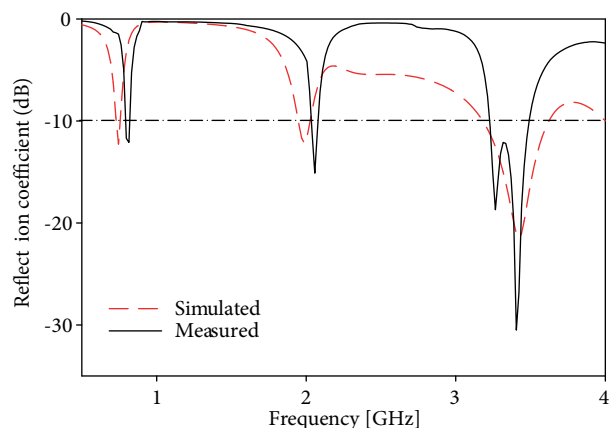
Figure 11. Measured and simulated reflection coefficient spectrum of the proposed antenna.

VSWR is one of the important parameters in antenna design which determines the impedance matching of the antenna. The antennas reported in the literature survey are defined by VSWRs less than 3 and reflection coefficients less than –6 dB. Generally, for a good impedance matching, VSWR should be less than 2 (VSWR $\leq$ 2). The simulated VSWR is illustrated in Figure 12. It is found that the antenna reveals a VSWR of 1.64 at 747 MHz, 1.65 at 1985 MHz, and 1.18 at 3422 MHz. The impedance matching is good across the operating bands.

The simulated far-field radiation pattern on the E-plane and H-plane for 747, 1980, and 3420 MHz are shown in the Figures 13a and 13b, respectively. The radiation pattern is simulated by setting $\phi = 90°$ for E-plane and $\phi = 0°$ for H-plane with respect to the θ value ranging from -180° to +180°. It is inferred that the antenna exhibits nearly dumbbell shape in E-plane (azimuth plane) and omnidirectional pattern in H-plane (elevation plane) for all the desired frequency bands.

The simulated 3D gain of the proposed antenna at three operating frequencies are shown in Figures 14a–14c. The gain is about –2.09 dBi at 747 MHz (low band), 2.05 dBi at 1985 MHz (middle band), and 1.489 dBi at 3422 MHz (high band).
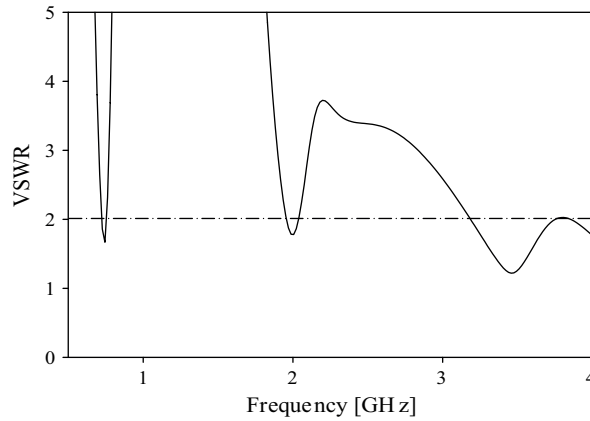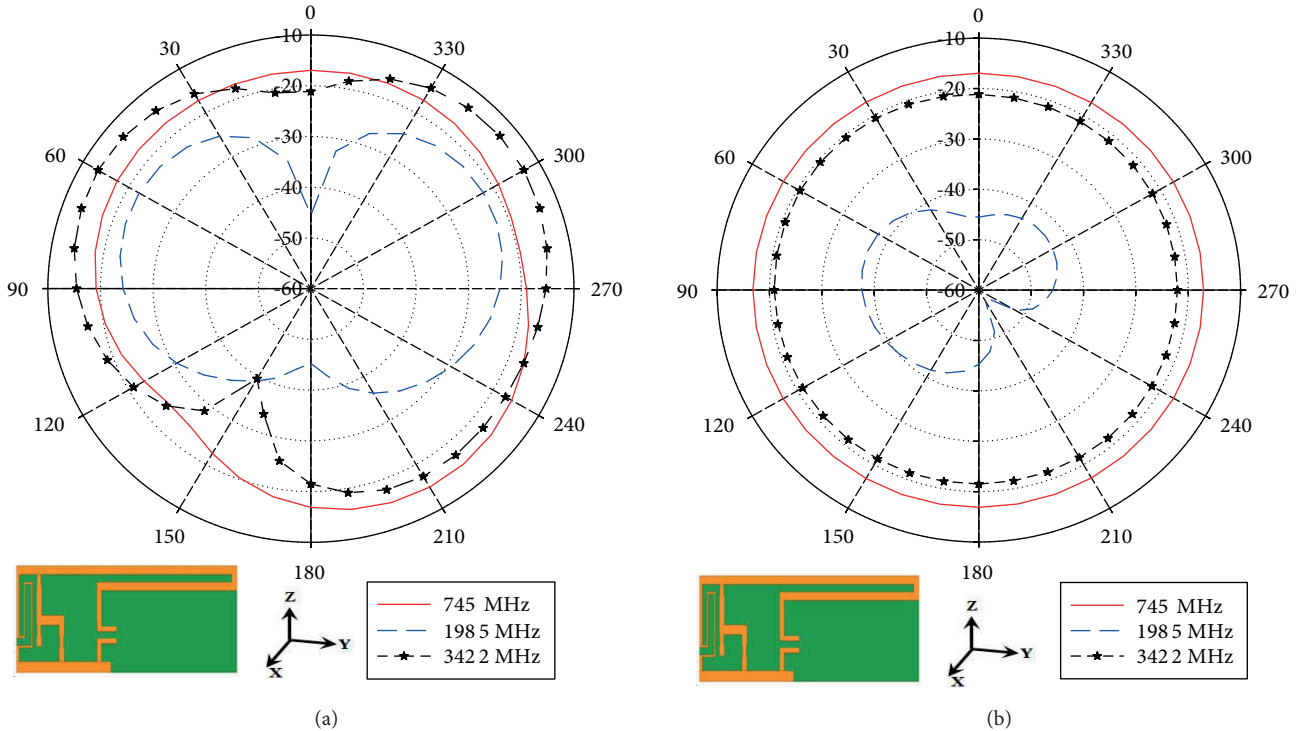
Figure 12. Plot of VSWR.

(a)

(b)

Figure 13. Far-field radiation pattern of the IFA (a) E-plane (azimuth plane), (b) H-plane (elevation plane).

The surface current distribution on the antenna at the corresponding frequencies of interest is illustrated in Figure 15. From Figure 15a, it is observed that the current density is higher at the folded radiating arm of the IFA, L-shaped strip, and the feeding arm at 747 MHz. The antenna has the maximum current of 5 A/m and minimum current of 0.676 A/m. The distributions of surface current at 1985 and 3422 MHz are presented in Figures 15b and 15c, respectively. It is also noted that there is only one current null on the radiating arm at 1985 and 3422 MHz and no such existence at 747 MHz. At 3422 MHz, the surface current is high in the radiating arm which increases the impedance bandwidth at the high-frequency band. The current density is found to be weak near the ground plane at three different resonant frequencies. In Table 2, the simulated and measured results are summarized.

Table 3 shows the comparison of the proposed inverted-F antenna with the previous LTE antennas which are considered from the literature survey. From Table 3, it is observed that the proposed antenna can operate in the triple band of LTE 700, LTE 2100, and LTE 3300 with compact size. It occupies less space in the printed circuit board while integrated with wireless devices.
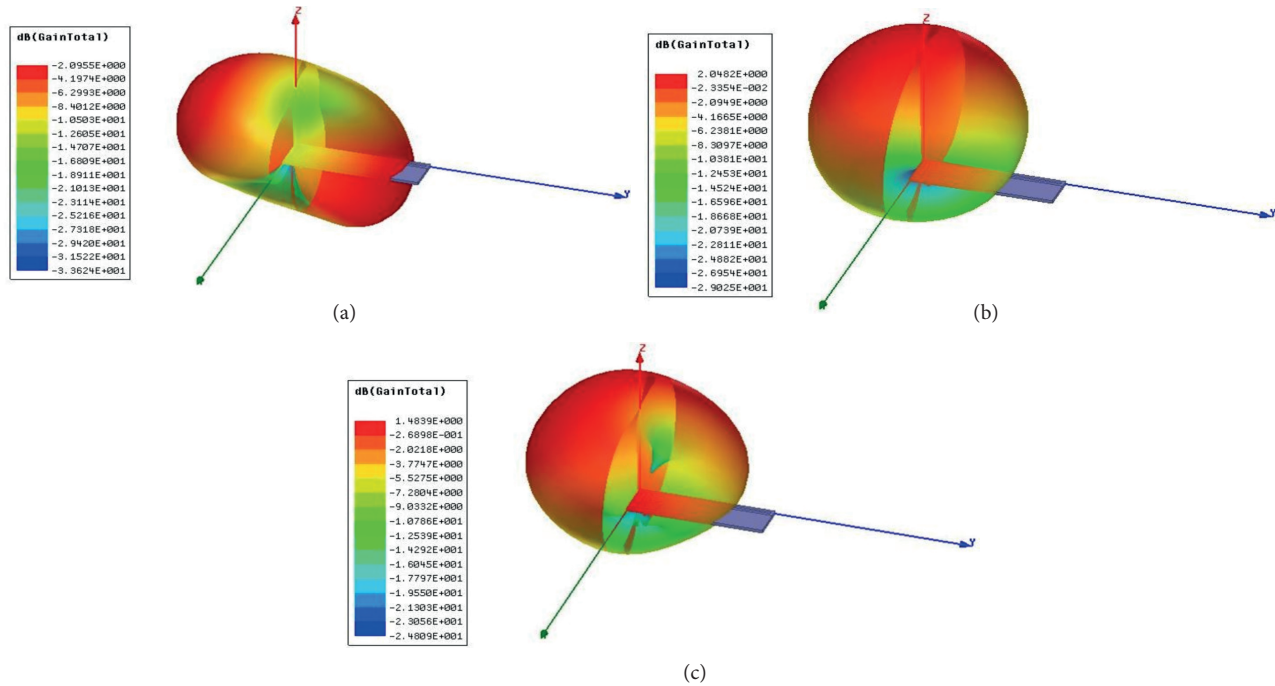

Figure 14. Simulated 3D gain of the IFA at (a) 747 MHz, (b) 1985 MHz, and (c) 3422 MHz.

Table 2. Summarized results of the proposed inverted-F antenna.

	Frequency (MHz)	Reflection coefficient (dB)	−10 dB BW (MHz)	% BW	Application
	747	−11.73	30	4.02	LTE 700
Simulated	1985	−12.10	80	4.04	LTE 2100
	3422	−21.46	470	13.74	LTE 3300
	795	−11.7	40	5.03	LTE 700
Measured	2050	−15.1	50	2.43	LTE 2100
	3405	−30.5	260	7.63	LTE 3300

6. Conclusion

In this work, a compact triple band inverted-F antenna for LTE-based wireless handheld devices has been presented. The proposed antenna has been manufactured and tested. The measured results show that the proposed antenna exhibits sufficient bandwidths of 40 MHz (5.03%), 50 MHz (2.43%), and 260 MHz (7.63%) at three operating frequencies of 795, 2050, and 3405 MHz. It can cover the LTE low band of 780–820 MHz (LTE 700), middle band of 2020–2070 MHz (LTE 2100), and high band of 3230–3490 MHz (LTE 3300), respectively.
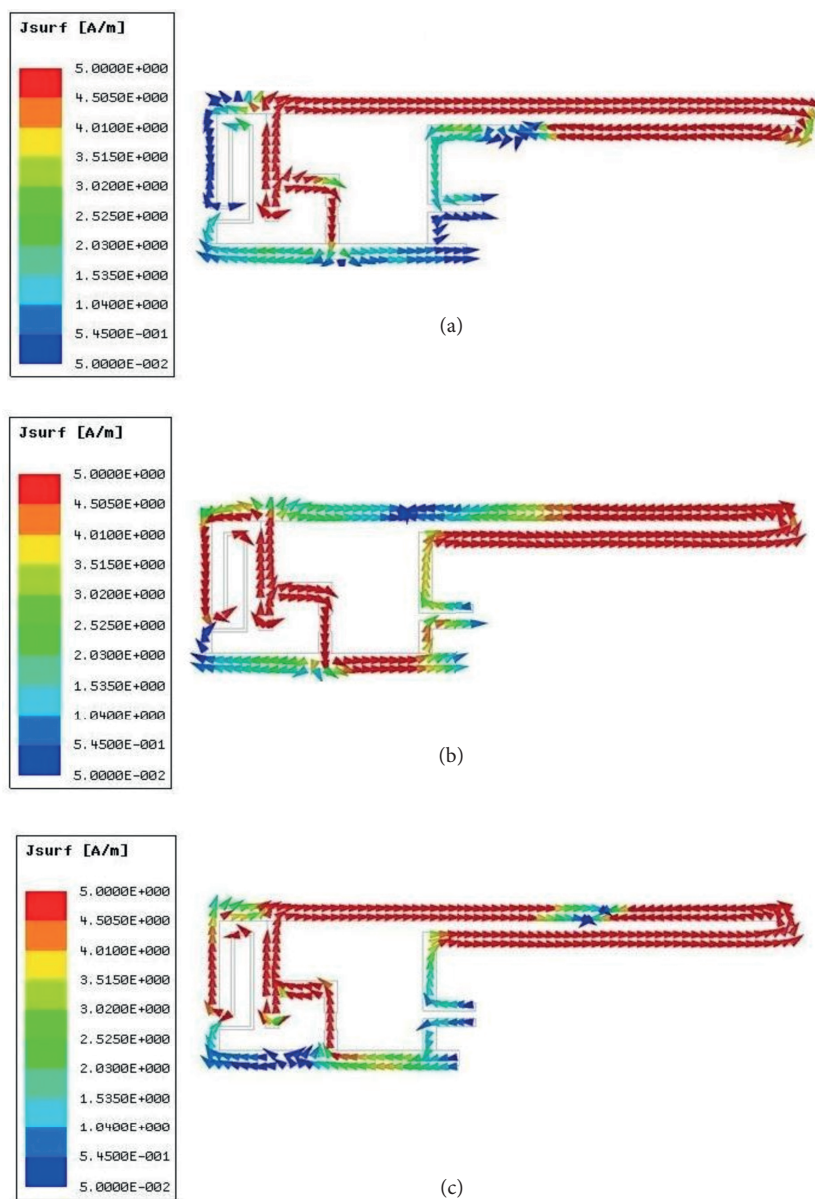
Figure 15. Vector surface current distributions of the IFA at (a) 747 MHz, (b) 1985 MHz, and (c) 3422 MHz.

Antenna has a compact size of $10 \times 35 \times 0.8$ mm^3. The results indicate that the antenna has acceptable performance for LTE operation. In addition, the suggested antenna is suitable for wireless handheld devices due to its ease of fabrication and low cost.

Table 3. Comparison of the proposed LTE antenna with reference antennas.

Antennas considered from references	No. of bands	Operating bands (MHz)	Resonant frequencies (MHz)	Size W*L*H (mm^3)
[17]	3	698–960	830	$10 \times 69 \times 1.6$
		1710–2200	1800	
		2600–2900	2800	
[18]	2		700	$40 \times 15 \times 0.8$
		698–960	2000	
		1653–3058	2500	
			3000	
[19]	3	745–787	760	$14 \times 15 \times 3.2$
		2300–2400	2000	
		2500 - 2690	2650	
[20]	3	920–960	950	$100 \times 6.5 \times 10$
		1900–2200	2100	
		3400–3800	3600	
Proposed antenna	3	780–820	795	$10 \times 35 \times 0.8$
		2020–2070	2050	
		3230–3490	3405	

Acknowledgment

References

[1] Palandöken M. Artificial materials based microstrip antenna design. In: Nasimuddin Nasimuddin, editor. Microstrip Antennas. London, UK: IntechOpen, Wiley Science, 2011. pp. 43-68. doi: 10.5772/14908

[2] Wu C, Wong K. Ultrawideband PIFA with a capacitive feed for penta-band folder-type mobile phone antenna. IEEE Transactions on Antennas and Propagation 2009; 57 (8): 2461-2464. doi: 10.1109/TAP.2009.2024571

[3] Li Y, Zhang Z, Chen W, Feng Z, Iskander MF. A quadband antenna with reconfigurable feedings. IEEE Antennas and Wireless Propagation Letters 2009; 8 (6): 1069-1071. doi: 10.1109/LAWP.2009.2031415

[4] Boyle KR, Steeneken PG. A five-band reconfigurable PIFA for mobile phones. IEEE Transactions on Antennas and Propagation 2007; 55 (11): 3300-3309. doi: 10.1109/TAP.2007.908822

[5] Chu F, Wong K. Simple folded monopole slot antenna for penta-band clamshell mobile phone application. IEEE Transactions on Antennas and Propagation 2009; 57 (11): 3680-3684. doi: 10.1109/TAP.2009.2025397

[6] Wong K, Chen S. Printed single-strip monopole using a chip inductor for penta-band WWAN Operation in the mobile phone. IEEE Transactions on Antennas and Propagation 2010; 58 (3): 1011-1014. doi: 10.1109/TAP.2009.2039324

[7] Wong KL, Chen WY. Small-size printed loop antenna for penta-band thin-profile mobile phone application. Microwave and Optical Technology Letters 2009; 51 (6): 1512-1517. doi: 10.1002/mop.24359

[8] Zheng M, Wang H, Hao Y. Internal hexa-band folded monopole/dipole/loop antenna with four resonances for mobile device. IEEE Transactions on Antennas and Propagation 2012; 60 (6): 2880-2885. doi: 10.1109/TAP.2012.2194687

[9] Park YK, Sung Y. A reconfigurable antenna for quad-band mobile handset applications. IEEE Transactions on Antennas and Propagation 2012; 60 (6): 3003-3006. doi: 10.1109/TAP.2012.2194672

[10] Li Y, Zhang Z, Zheng J, Feng Z, Iskander MF. A compact hepta-band loop-inverted F reconfigurable antenna for mobile phone. IEEE Transactions on Antennas and Propagation 2012; 60 (1): 389-392. doi: 10.1109/TAP.2011.2167949

[11] Ban Y, Sun S, Li P, Li JL, Kang K. Compact eight-band frequency reconfigurable antenna for LTE/WWAN tablet computer applications. IEEE Transactions on Antennas and Propagation 2014; 62 (1): 471-475. doi: 10.1109/TAP.2013.2287522

[12] Ali T, Khaleeq MM, Biradar RC. A multiband reconfigurable slot antenna for wireless applications. AEU - International Journal of Electronics and Communications 2018; 84: 273-280.

[13] Pan C, Horng T, Chen W, Huang C. Dual wideband printed monopole antenna for WLAN/WiMAX applications. IEEE Antennas and Wireless Propagation Letters 2007; 6: 149-151. doi: 10.1109/LAWP.2007.891957

[14] Komulainen M, Berg M, Palukuru VK, Jantunen H, Salonen E. Frequency-reconfigurable dual-band monopole antenna for mobile handsets. In: IEEE 2007 Antennas and Propagation Society International Symposium, Honolulu, HI USA; 2007. pp. 3289-3292. doi: 10.1109/APS.2007.4396239

[15] Deng C, Li Y, Zhang Z, Feng Z. Planar printed multi-resonant antenna for octa-band WWAN/LTE mobile handset. IEEE Antennas and Wireless Propagation Letters 2015; 14: 1734-1737. doi: 10.1109/LAWP.2015.2421335

[16] Zhang L, Ban Y, Sim C, Guo J, Yu Z.Parallel dual-loop antenna for WWAN/LTE metal-rimmed smartphone. IEEE Transactions on Antennas and Propagation 2018; 66 (3): 1217-1226. doi: 10.1109/TAP.2018.2796724

[17] Palandöken M. Dual broadband antenna with compact double ring radiators for IEEE 802.11 ac/b/g/n WLAN communication applications. Turkish Journal of Electrical Engineering & Computer Sciences 2017; 25 (2): 1326-1333. doi: 10.3906/elk-1507-121

[18] Wong K, Tsai C. Half-loop frame antenna for the LTE metal-casing tablet device. IEEE Transactions on Antennas and Propagation 2017; 65 (1): 71-81. doi: 10.1109/TAP.2016.2630716

[19] Chang S, Liao W. A broadband LTE/WWAN antenna design for tablet PC. IEEE Transactions on Antennas and Propagation 2012; 60 (9): 4354-4359. doi: 10.1109/TAP.2012.2207075

[20] Lu J, Wang Y. Internal uniplanar antenna for LTE/GSM/UMTS operation in a tablet computer. IEEE Transactions on Antennas and Propagation 2013; 61 (5): 2841-2846. doi: 10.1109/TAP.2013.2243693.

[21] Lin D, Chou J, Wu C, Li H. A novel miniaturized dual-layered LTE printed antenna for handheld devices. IEEE Antennas and Wireless Propagation Letters 2013; 12: 1680-1683. doi: 10.1109/LAWP.2013.2297693

[22] Yu K, Li Y, Luo X, Liu X. A modified E-shaped triple-band patch antenna for LTE communication applications. In: IEEE 2016 International Symposium on Antennas and Propagation (APSURSI); Fajardo, Puerto Rico: Online, 2016, pp. 295-296. doi:10.1109/APS.2016.7695856.

[23] Mohammad S. Sharawi, Printed MIMO Antenna Engineering. London, UK: Artech House, 2014.